Application of Multi-Input Volterra Theory to Nonlinear Multi-Degree-of-Freedom Aerodynamic Systems

Maciej Balajewicz,* Fred Nitzsche,† and Daniel Feszty‡
Carleton University, Ottawa, Ontario K1S 5B6, Canada

This paper presents a reduced-order-modeling approach for nonlinear, multi-degree-of-freedom aerodynamic systems using multi-input Volterra theory. The method is applied to a two-dimensional, 2 degree-of-freedom transonic airfoil undergoing simultaneous forced pitch and heave harmonic oscillations. The so-called Volterra cross kernels are identified and shown to successfully model the aerodynamic nonlinearities associated with the simultaneous pitch and heave motions. The improvements in accuracy over previous approaches that effectively ignored the cross kernels by using superposition are demonstrated.

I. Introduction

BECAUSE of the presence of aerodynamic nonlinearities in transonic aeroelasticity, computational fluid dynamics (CFD) has become the most reliable tool for its analysis. However, the large computational resources required for such high-fidelity analysis renders the approach undesirable, especially during the initial and conceptual design stages. As a result, there has been a great deal of interest in reduced-order models (ROMs) of the transonic nonlinear system [1–3]. A ROM is a simplified mathematical model that captures most of the physics of the more complex system under investigation. Among the many ROM methods available, the most popular include proper orthogonal decomposition, harmonic balance, and the Volterra series. Although research into the Volterra series as a ROM for the transonic aerodynamic system has been significant [2–11], several critical issues remain unsolved. In his recent review paper, Silva [3] suggested that the application of the Volterra theory to multi-degree-of-freedom systems has been incomplete. He states that "An important issue that needs to be addressed is the simultaneous excitation of multiple degrees of freedom to properly identify any nonlinear crosscoupling of the degrees of freedom." All previous applications of the Volterra series to multi-degree-of-freedom aerodynamic systems have been limited to the identification of aerodynamic nonlinearities resulting from individual perturbations of structural modes. Determination of total lift and moment for simultaneous motions required the superposition of the individual nonlinear responses. However, as suggested by Silva [3], the nonlinear nature of the system renders the principle of superposition invalid.

This paper attempts to address this issue by proposing the multi-input Volterra series as a viable ROM method for nonlinear multi-degree-of-freedom aerodynamic systems. The multi-input Volterra series is well suited for this purpose and has been success-

fully used by researchers in other disciplines [12–16]. The multi-input Volterra series differs from the classical single-input Volterra series through its inclusion of Volterra cross kernels. These cross kernels capture the coupling dynamics between the degrees of freedom of the nonlinear system. The applicability of the multi-input Volterra series to nonlinear aerodynamic systems is illustrated by modeling the transonic, unsteady, two-dimensional, 2 DOF airfoil.

II. Volterra Theory

The Volterra theory of nonlinear systems is quite mature and several texts are available [17,18]. It was first applied to nonlinear engineering problems by Wiener [19] and first applied to subsonic and transonic aerodynamic systems by Tromp and Jenkins [4] and Silva [5], respectively. This section provides a brief summary of the Volterra theory of single- and multi-input nonlinear systems both in continuous and discrete-time domains.

A. Single-Input Volterra Theory

The output $y(t)$, of a continuous-time, causal, time-invariant, fading memory, nonlinear system Ψ, due to a single-input $x(t)$

$$y(t) = \Psi\{x(t)\} \tag{1}$$

can be modeled using the pth-order Volterra series

$$
\begin{aligned}
y(t) &= \sum_{i=1}^{p} \mathbb{H}_i \\
&= \int_{-\infty}^{t} H_1(t-\tau)x(\tau)\,d\tau \\
&\quad + \int_{-\infty}^{t}\int_{-\infty}^{t} H_2(t-\tau_1, t-\tau_2)x(\tau_1)x(\tau_2)\,d\tau_1\,d\tau_2 \\
&\quad \vdots \\
&\quad + \int_{-\infty}^{t}\cdots\int_{-\infty}^{t} H_p(t-\tau_1,\ldots,t-\tau_p)\prod_{i=1}^{p}\{x(\tau_i)\,d\tau_i\}
\end{aligned} \tag{2}
$$

where the pth-order Volterra operator $\mathbb{H}_p$, is defined as a p-fold convolution between the input $x(t)$ and the pth-order Volterra kernel $H_p(t,\ldots,t)$. The identification of Volterra kernels is key to the synthesis of a Volterra ROM. However, analytical derivations of the Volterra kernels in continuous time are only possible if analytical, closed-form expressions of the input–output relationship of the nonlinear system Ψ are available. Unfortunately, many engineering applications of interest including aerodynamic applications lack such closed-form formulations and, instead, rely on numerical solutions of the nonlinear system Ψ. As a result, identification of the Volterra kernels involves the processing of discrete-time outputs due to

*Graduate Student, Department of Mechanical and Aerospace Engineering; currently Graduate Student, Department of Mechanical Engineering and Materials Science, Duke University, Durham, North Carolina 27708; maciej.balajewicz@duke.edu. Student Member AIAA.
†Professor, Department of Mechanical and Aerospace Engineering. Senior Member AIAA.
‡Assistant Professor, Department of Mechanical and Aerospace Engineering. Member AIAA.

specifically tailored training inputs. Consequently, the discrete-time version of the Volterra series using discrete-time Volterra operators and kernels is preferred. For a uniformly sampled, discrete-time representation of the system

$$y[n] = \Psi\{x[n]\} \qquad (3)$$

where for $n = 0, 1, \ldots, N$

$$x[n] = x(t)|_{t=n\Delta T} = x(n\Delta T)$$
$$y[n] = y(t)|_{t=n\Delta T} = y(n\Delta T) \qquad (4)$$

The output $y[n]$ of a nonlinear system Ψ due to a single input $x[n]$ can be modeled using the pth-order, discrete-time, Volterra series

$$
\begin{aligned}
y[n] &= \sum_{i=1}^{p} \mathbb{H}_i \\
&= \sum_{k=0}^{n} H_1[n-k]x[k] \\
&\quad + \sum_{k_1=0}^{n}\sum_{k_2=0}^{n} H_2[n-k_1, n-k_2]x[k_1]x[k_2] \\
&\quad \vdots \\
&\quad + \sum_{k_1=0}^{n}\cdots\sum_{k_p=0}^{n} H_p[n-k_1,\cdots,n-k_p]\prod_{i=1}^{p} x[k_i]
\end{aligned}
\qquad (5)
$$

where the pth-order, discrete-time Volterra operator $\mathbb{H}_p$ is defined as a p-fold discrete-time convolution between the input $x[n]$ and the pth-order, discrete-time Volterra kernel $H_p[n, \ldots, n]$. Because of the exponentially increasing difficulty inherent in identifying higher-order, discrete-time Volterra kernels, most applications, including aerodynamic ones, use a truncated, second-order ($p = 2$) Volterra series

$$y[n] = \sum_{k=0}^{n} H_1[n-k]x[k] + \sum_{k_1=0}^{n}\sum_{k_2=0}^{n} H_2[n-k_1, n-k_2]x[k_1]x[k_2] \qquad (6)$$

Unfortunately, such a low-ordered truncation of the Volterra series restricts its ROM capability to weakly nonlinear systems only. Although precise and generally applicable definitions of weakness are lacking, the general consensus is that a weakly nonlinear system is one whose output only weakly diverges from the output predicted by linearized models.

B. Single-Input Volterra Kernel Identification

In this paper, Silva's familiar impulse identification method for the first- and second-order discrete-time Volterra kernels is used:

$$\xi H_1[n] = 2\Psi\{\delta[n]\} + \tfrac{1}{2}\Psi\{2\delta[n]\} \qquad (7)$$

$$
\begin{aligned}
\sum_{k=0}^{N} (2\xi^2 H_2[n, n-k] &= \Psi\{\delta[n] + \delta[n-k]\} \\
&\quad - \Psi\{\delta[n]\} - \Psi\{\delta[n-k]\})
\end{aligned}
\qquad (8)
$$

where $\delta[n]$ is an impulse function of magnitude ξ

$$\delta[n] = \begin{cases} \xi & n = 0 \\ 0 & n \neq 0 \end{cases} \qquad (9)$$

The identification of the first-order kernel $H_1[n]$ is straightforward. Only two outputs due to inputs $\delta[n]$ and $2\delta[n]$ are required. The identification of the second-order kernel $H_2[n, n]$ is more involved because multiple outputs due to inputs $\delta[n]$ and $\delta[n-k]$ for $k = 0, 1, \ldots, N$ must be computed. Because of symmetry, for all k

$$H_2[n, n-k] = H_2[n-k, n] \qquad (10)$$

C. Multi-Input Volterra Theory

The output $y(t)$ of a continuous-time, causal, time-invariant, fading memory, nonlinear system Ψ due to m inputs

$$y(t) = \Psi\{x_1(t), x_2(t), \ldots, x_m(t)\} \qquad (11)$$

can be modeled using the pth-order, multi-input Volterra series

$$
\begin{aligned}
y(t) &= \sum_{i=1}^{p} \mathbb{H}_i^m \\
&= \sum_{j=1}^{m}\left\{\int_{-\infty}^{t} H_1^j(t-\tau)x_j(\tau)\,d\tau\right\} \\
&\quad + \sum_{j_1=1}^{m}\sum_{j_2=1}^{m}\left\{\int_{-\infty}^{t}\int_{-\infty}^{t} H_2^{j_1 j_2}(t-\tau_1, t-\tau_2)x_{j_1}(\tau_1)x_{j_2}(\tau_2)\,d\tau_1\,d\tau_2\right\} \\
&\quad \vdots \\
&\quad + \sum_{j_1=1}^{m}\cdots\sum_{j_p=1}^{m}\left\{\int_{-\infty}^{t}\cdots\int_{-\infty}^{t} H_p^{j_1\cdots j_p}(t-\tau_1, \ldots, t-\tau_p)\right. \\
&\qquad\qquad \left. \times \prod_{i=1}^{p}\{x_{j_i}(\tau_i)\,d\tau_i\}\right\}
\end{aligned}
\qquad (12)
$$

where the pth-order, multi-input Volterra operator $\mathbb{H}_p^m$ is defined as a m^p-fold summation of p-fold convolution integrals between the various combinations of inputs $x_1(t), x_2(t), \ldots, x_m(t)$, and the pth-order, multi-input Volterra kernel $H_p^{j_1\cdots j_p}(t, \ldots, t)$. Notice the appearance of superscripts on the pth-order, multi-input Volterra kernel $H_p^{j_1\cdots j_p}(t, \ldots, t)$. These superscripts identify to which inputs the kernel corresponds. For example, a third-order kernel $H_3^{512}(t, t, t)$ corresponds to inputs $x_5(t)$, $x_1(t)$, and $x_2(t)$. Volterra kernels $H_p^{j_1\cdots j_p}(t, \ldots, t)$, where $j_1 = j_2 = \cdots = j_p$, are called Volterra *direct* kernels. Volterra kernels with superscripts that do not match are called Volterra *cross* kernels. The presence of these Volterra cross kernels differentiates the multi-input Volterra series from the single-input Volterra series summarized in Sec. II.A.

For a uniformly sampled, discrete-time representation of the system Ψ

$$y[n] = \Psi\{x_1[n], x_2[n], \ldots, x_m[n]\} \qquad (13)$$

where $n = 0, 1, \ldots, N$

$$\sum_{i=1}^{m}\{x_i[n] = x_i(t)|_{t=n\Delta T} = x_i(n\Delta T)\}$$
$$y[n] = y(t)|_{t=n\Delta T} = y(n\Delta T) \qquad (14)$$

The output $y[n]$ of a nonlinear system Ψ due to m inputs can be modeled using the pth-order, discrete-time, multi-input Volterra series

$$
\begin{aligned}
y[n] &= \sum_{i=1}^{p} \mathbb{H}_i^m \\
&= \sum_{j=1}^{m}\left\{\sum_{k=0}^{n} H_1^j[n-k]x_j[k]\right\} \\
&\quad + \sum_{j_1=1}^{m}\sum_{j_2=1}^{m}\left\{\sum_{k_1=0}^{n}\sum_{k_1=0}^{n} H_2^{j_1 j_2}[n-k_1, n-k_2]x_{j_1}[k_1]x_{j_2}[k_2]\right\} \\
&\quad \vdots \\
&\quad + \sum_{j_1=1}^{m}\cdots\sum_{j_p=1}^{m}\left\{\sum_{k_1=0}^{n}\cdots\sum_{k_p=0}^{n} H_p^{j_1\cdots j_p}[n-k_1,\cdots,n-k_p]\right. \\
&\qquad\qquad \left. \times \prod_{i=1}^{p}\{x_{j_i}[k_i]\}\right\}
\end{aligned}
\qquad (15)
$$

where the pth-order, discrete-time, multi-input Volterra operator $\mathbb{H}_p^m$ is defined as a m^p-fold summation of p-fold discrete-time

convolutions between the various combinations of inputs $x_1[n]$, $x_2[n], \ldots, x_m[n]$ and the pth-order, multi-input, discrete-time Volterra kernel $H_p^{j_1 \cdots j_p}[n, \ldots, n]$. The difficulties associated with the identification of higher-order, multi-input, discrete-time Volterra direct and cross kernels are identical to those associated with the identification of higher-order, single-input, discrete-time Volterra kernels. In other words, only a second-order ($p = 2$), multi-input Volterra series is practical

$$y[n] = \sum_{j=1}^{m} \left\{ \sum_{k=0}^{n} H_1^j[n - \tau]x_j[k] \right\}$$
$$+ \sum_{j_1=1}^{m} \sum_{j_2=1}^{m} \left\{ \sum_{k_1=0}^{n} \sum_{k_1=0}^{n} H_2^{j_1 j_2}[n - k_1, n - k_2]x_{j_1}[k_1]x_{j_2}[k_2] \right\} \quad (16)$$

D. Multi-Input Volterra Kernel Identification

As in the previous section dealing with the single-input Volterra series, we use the impulse identification method for the first- and second-order direct and cross kernels:

$$\sum_{j=1}^{m} \left(\xi_j H_1^j[n] = 2\Psi\{\delta_j[n]\} + \frac{1}{2}\Psi\{2\delta_j[n]\} \right) \quad (17)$$

$$\sum_{j_1=1}^{m} \sum_{j_2=1}^{m} \left\{ \sum_{k=0}^{N} (2\xi_{j_1}\xi_{j_2} H_2^{j_1 j_2}[n, n - k] = \Psi\{\delta_{j_1}[n] + \delta_{j_2}[n - k]\} \right.$$
$$\left. - \Psi\{\delta_{j_1}[n]\} - \Psi\{\delta_{j_2}[n - k]\}) \right\}$$
$$(18)$$

where $\delta_j[n]$ is an impulse function corresponding to the jth input

$$\delta_j[n] = \begin{cases} \xi_j & n = 0 \\ 0 & n \neq 0 \end{cases} \quad (19)$$

Because of symmetry, for all k

$$H_2^{j_1 j_2}[n, n - k] = H_2^{j_1 j_2}[n - k, n] \quad \text{for } j_1 = j_2$$
$$H_2^{j_1 j_2}[n, n - k] = H_2^{j_2 j_1}[n - k, n] \quad \text{for } j_1 \neq j_2 \quad (20)$$

III. Multi-Input Volterra Reduced-Order Model of 2 Degree-of-Freedom Airfoil

The 2 DOF oscillations in both pitch α and heave h fully characterize the unsteady motion of a two-dimensional airfoil of chord c immersed in transonic flow, as illustrated in Fig. 1a. The aerodynamics of such an airfoil are described using the coefficient of lift C_L and moment C_M, as shown in Fig. 1b. However, for the sake of brevity, in this paper we limit our discussion to the aerodynamic moment output only. Unlike the pitch degree of freedom, only a heave velocity $\dot{h}$ is capable of producing aerodynamic loading. Therefore, from a Volterra series ROM point of view, it is more appropriate to use $\dot{h}$, instead of h, as one of the inputs to the aerodynamic system:

$$C_M[n] = \text{CFD}\{\alpha[n], \dot{h}[n]\} \quad (21)$$

To capture the nonlinear effects of the transonic flow regime, the traditional Volterra ROM approach has been to superimpose two second-order Volterra ROMs, one per each degree of freedom:

$$C_M[n] = \sum_{k=0}^{n} H_1^\alpha[n - k]\alpha[k] + \sum_{k=0}^{n} H_1^h[n - k]\dot{h}[k]$$
$$+ \sum_{k_1=0}^{n} \sum_{k_2=0}^{n} H_2^{\alpha\alpha}[n - k_1, n - k_2]\alpha[k_1]\alpha[k_2]$$
$$+ \sum_{k_1=0}^{n} \sum_{k_2=0}^{n} H_2^{\dot{h}\dot{h}}[n - k_1, n - k_2]\dot{h}[k_1]\dot{h}[k_2] \quad (22)$$

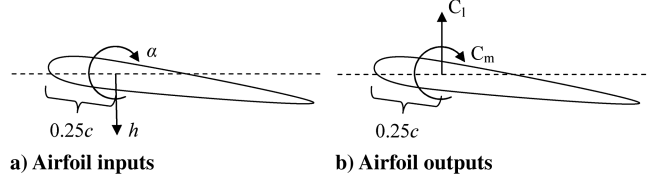a) Airfoil inputs   b) Airfoil outputs

Fig. 1   The 2 DOF, two-dimensional airfoil system.

where H_1^α, $H_2^{\alpha\alpha}$ and $H_1^{\dot{h}}$, $H_2^{\dot{h}\dot{h}}$ are the first- and second-order direct Volterra kernels corresponding to the pitch and heave degrees of freedom. However, as suggested by Silva [3], the nonlinearities of the system render the superposition principle invalid. The multi-input Volterra series is a more appropriate ROM for this system due to its inclusion of Volterra cross kernels, which are capable of modeling the nonlinearities associated with the simultaneous perturbation of the pitch and heave degrees of freedom. The second-order, multi-input Volterra series ROM of this system is formed by setting $j_1 = \alpha$ and $j_2 = \dot{h}$ in Eq. (16):

$$C_M[n] = \sum_{k=0}^{n} H_1^\alpha[n - k]\alpha[k] + \sum_{k=0}^{n} H_1^{\dot{h}}[n - k]\dot{h}[k]$$
$$+ \sum_{k_1=0}^{n} \sum_{k_2=0}^{n} H_2^{\alpha\alpha}[n - k_1, n - k_2]\alpha[k_1]\alpha[k_2]$$
$$+ \sum_{k_1=0}^{n} \sum_{k_2=0}^{n} H_2^{\dot{h}\dot{h}}[n - k_1, n - k_2]\dot{h}[k_1]\dot{h}[k_2]$$
$$+ \sum_{k_1=0}^{n} \sum_{k_2=0}^{n} H_2^{\alpha\dot{h}}[n - k_1, n - k_2]\alpha[k_1]\dot{h}[k_2]$$
$$+ \sum_{k_1=0}^{n} \sum_{k_2=0}^{n} H_2^{\dot{h}\alpha}[n - k_1, n - k_2]\dot{h}[k_1]\alpha[k_2] \quad (23)$$

where $H_2^{\alpha\dot{h}}$ and $H_2^{\dot{h}\alpha}$ are the second-order Volterra cross kernels. All the required first- and second-order Volterra direct and cross kernels in Eq. (23) are identified using the impulse identification method summarized in Sec. II.D:

$$\xi_\alpha H_1^\alpha[n] = 2\text{CFD}\{\delta_\alpha[n]\} + \frac{1}{2}\text{CFD}\{2\delta_\alpha[n]\}$$
$$\xi_{\dot{h}} H_1^{\dot{h}}[n] = 2\text{CFD}\{\delta_{\dot{h}}[n]\} + \frac{1}{2}\text{CFD}\{2\delta_{\dot{h}}[n]\} \quad (24)$$

$$\sum_{k=0}^{N} (2\xi_\alpha^2 H_2^{\alpha\alpha}[n, n - k] = \text{CFD}\{\delta_\alpha[n] + \delta_\alpha[n - k]\}$$
$$- \text{CFD}\{\delta_\alpha[n]\} - \text{CFD}\{\delta_\alpha[n - k]\})$$

$$\sum_{k=0}^{N} (2\xi_{\dot{h}}^2 H_2^{\dot{h}\dot{h}}[n, n - k] = \text{CFD}\{\delta_{\dot{h}}[n] + \delta_{\dot{h}}[n - k]\}$$
$$- \text{CFD}\{\delta_{\dot{h}}[n]\} - \text{CFD}\{\delta_{\dot{h}}[n - k]\})$$

$$\sum_{k=0}^{N} (2\xi_\alpha\xi_{\dot{h}} H_2^{\alpha\dot{h}}[n, n - k] = \text{CFD}\{\delta_\alpha[n] + \delta_{\dot{h}}[n - k]\}$$
$$- \text{CFD}\{\delta_\alpha[n]\} - \text{CFD}\{\delta_{\dot{h}}[n - k]\})$$

$$\sum_{k=0}^{N} (2\xi_{\dot{h}}\xi_\alpha H_2^{\dot{h}\alpha}[n, n - k] = \text{CFD}\{\delta_{\dot{h}}[n] + \delta_\alpha[n - k]\}$$
$$- \text{CFD}\{\delta_{\dot{h}}[n]\} - \text{CFD}\{\delta_\alpha[n - k]\}) \quad (25)$$

where $\delta_\alpha[n]$ and $\delta_{\dot{h}}[n]$ are impulse functions corresponding to the pitch α and heave velocity $\dot{h}$ inputs:

$$\delta_\alpha[n] = \begin{cases} \xi_\alpha & n = 0 \\ 0 & n \neq 0 \end{cases} \qquad \delta_{\dot{h}}[n] = \begin{cases} \xi_{\dot{h}} & n = 0 \\ 0 & n \neq 0 \end{cases} \quad (26)$$

IV. Description of Test Case

To demonstrate the applicability of the multi-input Volterra series as a ROM method for nonlinear, multi-degree-of-freedom aerodynamic systems, we chose to model a symmetric NACA 0012 airfoil oscillating about a nonzero static angle of attack:

$$\alpha = \alpha_0 + \bar{\alpha}\sin(2k_\alpha\tau) \qquad \dot{h} = \bar{\dot{h}}\sin(2k_{\dot{h}}\tau) \qquad (27)$$

where $k = \omega c/2U_\infty$, $\tau = U_\infty t/c$. The static and dynamic pitch amplitudes, α_0 and $\bar{\alpha}$, have units of degrees, whereas the dynamic heave velocity amplitude $\bar{\dot{h}}$ is dimensionless because $\dot{h} = d(h/c)/d\tau$. When assigning values to the parameters in Eq. (27), several requirements must be satisfied:

1) For the prescribed motion, reliable experimental data should exist to validate the CFD output.

2) The nonlinear lift and moment response due to these motions must be weakly nonlinear.

To the authors' knowledge, no experimental data for simultaneously forced pitch and heave oscillations at transonic conditions exist. However, the experimental data are numerous for forced pitch motions alone. An often-cited experimental data set of lift and moment values for forced pitch motions at transonic conditions is the 1982 AGARD Compendium of Unsteady Aerodynamic Measurements [20]. This AGARD report introduces the so-called CT2 test case:

$$\alpha = 3.16 \text{ deg} + 4.59 \text{ deg} \sin(2k_\alpha\tau) \qquad (28)$$

at a Mach number M of 0.6 and a pitch reduced frequency of $k_\alpha = 0.0811$. The aerodynamics of this test case are characterized by the formation of a strong and highly dynamic shock wave experiencing Tijdeman and Seebass's [21] type-B shock motion. Unfortunately, strong and highly dynamic shock waves are known to produce highly nonlinear lift and moment response. Because a second-order Volterra ROM can only handle weak nonlinearities, the dynamic pitch motion must be decreased so that weaker, less-dynamic shock waves are formed. Observing the pressure contours from the AGARD reports, this condition is satisfied at dynamic pitch amplitudes of approximately 1 deg.

Because the aim of this paper is to present a method of modeling multi-degree-of-freedom aerodynamic systems using the multi-input Volterra series, the airfoil motion must include heave. The main difference between the application of the multi-input Volterra series over the single-input Volterra series is the identification of cross kernels. Because we wish to focus on these cross kernels, it is helpful to select a dynamic heave velocity amplitude that would yield a heave velocity direct kernel approximately equal in magnitude to the pitch direct kernel. After several systematic CFD runs, it was found that a dimensionless heave velocity amplitude of 0.018 would achieve this requirement. Hence, the following 2 DOF motion was chosen:

$$\alpha = 3.16 \text{ deg} + 1 \text{ deg} \sin(2k_\alpha\tau) \qquad \dot{h} = 0.018\sin(2k_{\dot{h}}\tau) \quad (29)$$

where $M = 0.6$, $k_\alpha = 0.0811$, and $k_h = 0.8k_\alpha$.

V. CFD Using the Carleton Multiblock Solver

All CFD results presented in this paper were carried out using the Carleton multiblock (CMB) CFD code. The CMB code is a derivative of a code originally developed at the University of Glasgow, specifically tailored for transonic, time-marching aero-elastic analysis. The aerodynamics of the airfoil were modeled using the inviscid Euler equations. For further details, refer to Dubuc et al. [22] and Badcock et al. [23].

The NACA 0012 airfoil domain was discretized using a C-type 180×33 Euler grid with 130 nodes on the airfoil. The surface nodes were at a distance of approximately $0.001c$ off the airfoil surface. The mesh extended into the far field approximately $10c$ in all directions. The unsteady solutions were solved using a dimensionless time step $\Delta\tau = 1.96$, which corresponds to 20 time steps per period of pitch oscillation. This choice of mesh and time step was based on several

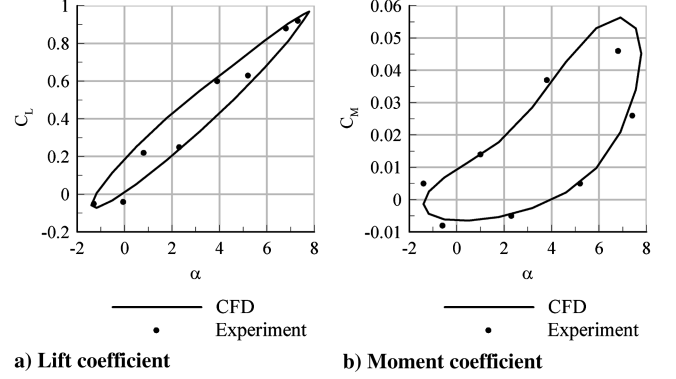a) Lift coefficient   b) Moment coefficient

Fig. 2   CFD validation of AGARD test case.

mesh refinement studies carried out by Dubuc et al. [22], which showed that no significant accuracy improvements are gained at higher spatial or temporal discretizations.

Figure 2 compares the experimental and CFD outputs of the AGARD test case as described by Eq. (28); very good agreement was obtained. Errors are likely associated with the neglect of viscous forces and uncertainties in the experimental data [22,23].

VI. Results and Discussion

A. Volterra Kernel Identification

As stated in the theoretical derivation of the Volterra series in Sec. III, the first- and second-order kernels identified using Eqs. (24) and (25) are illustrated in Figs. 3 and 4, respectively. From sensitivity studies summarized in Secs. VI.C and VI.D, both the first- and second-order kernels are identified using $\Delta\tau = 2$, $\xi_\alpha = 0.5$ deg, and $\xi_{\dot{h}} = 0.009$. On a single Intel Pentium 3.2 GHz desktop machine running Red Hat 2.6.9 with 1 GB of RAM, the identification of a single first-order and a single second-order kernel requires approximately 51 s (0.85 min) and 550 s (9.1 min) of CPU time, respectively. Because of the quickly decaying nature of the second-order kernels, only the first 10 terms are identified, that is, in Eq. (25), $N = 10$.

B. Multi-Input Volterra Reduced-Order Model of Transonic Airfoil

Figures 5a and 5b illustrate the CFD and Volterra ROM moment coefficient outputs due to the individual application of the pitch and heave inputs of Eq. (31), respectively. It should be noted that the moment coefficient due to the steady pitch of 3.16 deg has been subtracted from the unsteady results presented in this section. In both cases, the Volterra ROM, which includes both the first- and second-order kernels, performs better at modeling the nonlinear CFD output.

Figure 6 illustrates the CFD moment coefficient output due to the simultaneous application of pitch and heave inputs CFD$\{\alpha + h\}$ and the superposition of outputs due to individual application of the pitch and heave inputs CFD$\{\alpha\}$ + CFD$\{h\}$. We can clearly verify that, due to the nonlinear nature of the aerodynamic system, the superposition of the individual outputs does not accurately predict the output due to the simultaneous application of inputs. Note the clear presence of a
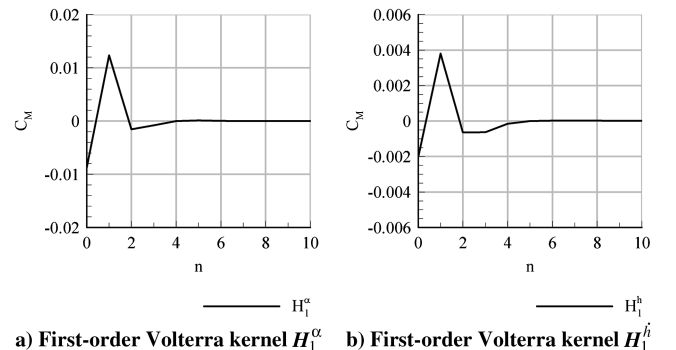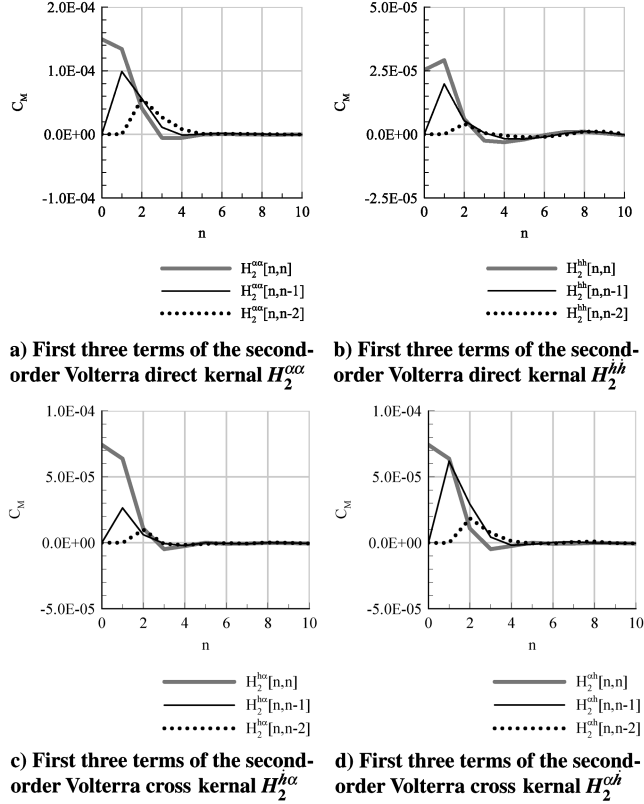

a) First-order Volterra kernel H_1^α b) First-order Volterra kernel $H_1^{\dot{h}}$

Fig. 3   First-order Volterra kernels of the transonic airfoil.

a) First three terms of the second-order Volterra direct kernal $H_2^{\alpha\alpha}$

b) First three terms of the second-order Volterra direct kernal $H_2^{\dot{h}\dot{h}}$

c) First three terms of the second-order Volterra cross kernal $H_2^{\dot{h}\alpha}$

d) First three terms of the second-order Volterra cross kernal $H_2^{\alpha\dot{h}}$

Fig. 4   Second-order Volterra kernels of the transonic airfoil.

a) Moment coefficient output due to pitch input

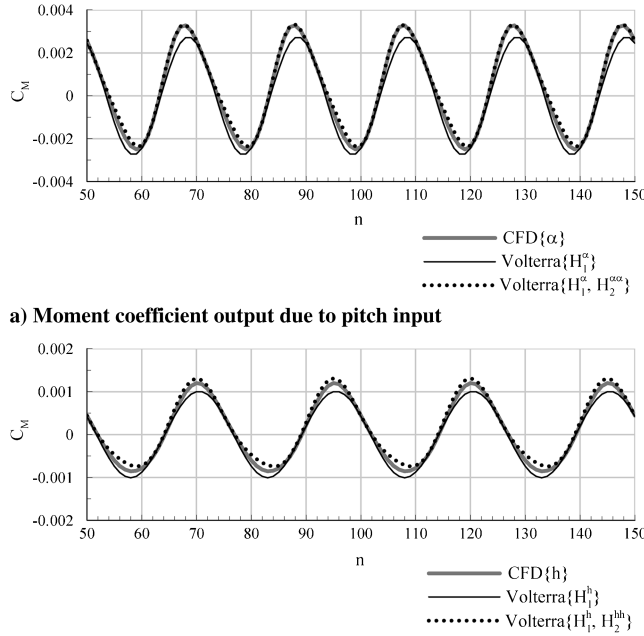b) Moment coefficient output due to heave input

Fig. 5   Moment coefficient outputs due to individual application of pitch and heave motions.

beat frequency in the aerodynamic moment coefficient resulting from the input frequency ratio being nearly equal to one. Figure 7 compares the simultaneous CFD{$\alpha + h$} and superimposed CFD{α} + CFD{h} outputs with a Volterra ROM that only includes the direct kernels H_1^{α}, $H_1^{\dot{h}}$, $H_2^{\alpha\alpha}$, and $H_2^{\dot{h}\dot{h}}$. As expected, the superimposed output CFD{α} + CFD{h} is well predicted, but the simultaneous output CFD{$\alpha + h$} is not.

Figure 8 shows how the inclusion of cross kernels $H_2^{\dot{h}\alpha}$ and $H_2^{\alpha\dot{h}}$ significantly improves the accuracy of the Volterra ROM in modeling the simultaneous response.
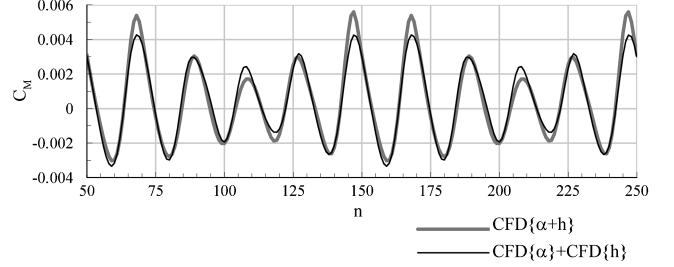

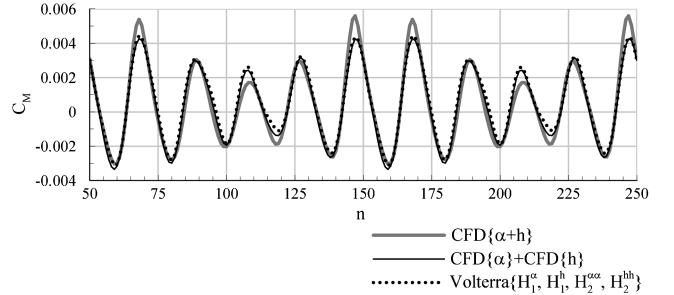**Fig. 6   Superimposed and simultaneous pitch and heave motion outputs.**

Fig. 7   Volterra ROM using direct kernels only against superimposed and simultaneous pitch and heave motion CFD output.
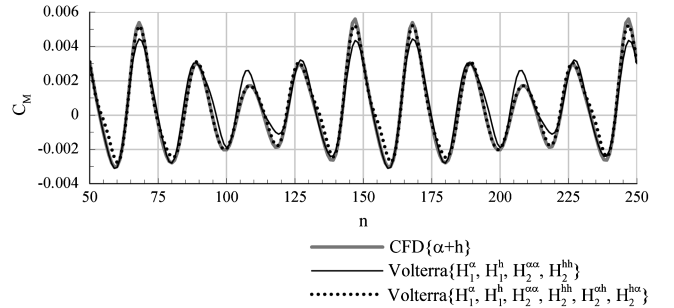

Fig. 8   Volterra ROM using direct kernels only and a Volterra ROM using both direct and cross kernels against simultaneous pitch and heave motion CFD output.

We can quantify the modeling performance of the Volterra ROMs using the L^2 relative error norm, defined as

$$\%\text{Error} = \sqrt{\frac{(\text{CFD}\{\alpha + h\} - \text{Volterra ROM})^2}{\text{CFD}\{\alpha + h\}^2}} \times 100 \qquad (30)$$

Error norms for the various Volterra ROMs covered in this section are summarized in Table 1. As expected, the inclusion of the cross kernels significantly increases the accuracy of the Volterra ROM.

Figure 9 shows the frequency content of the CFD{$\alpha + h$} output and the various Volterra kernels that make up the Volterra ROMs. The first-order kernels H_1^{α} and $H_1^{\dot{h}}$ capture the fundamental, linear output frequencies $k/k_{\alpha} = 1$ and $k/k_{\alpha} = 0.8$. The second-order, direct kernels $H_2^{\alpha\alpha}$ and $H_2^{\dot{h}\dot{h}}$ capture the first three integer harmonics $k/k_{\alpha} = 2$ (i.e., $k/k_{\alpha} = 2 \times 1$), $k/k_{\alpha} = 1.6$ (i.e., $k/k_{\alpha} = 2 \times 0.8$), and

Table 1   Volterra ROM modeling error norms

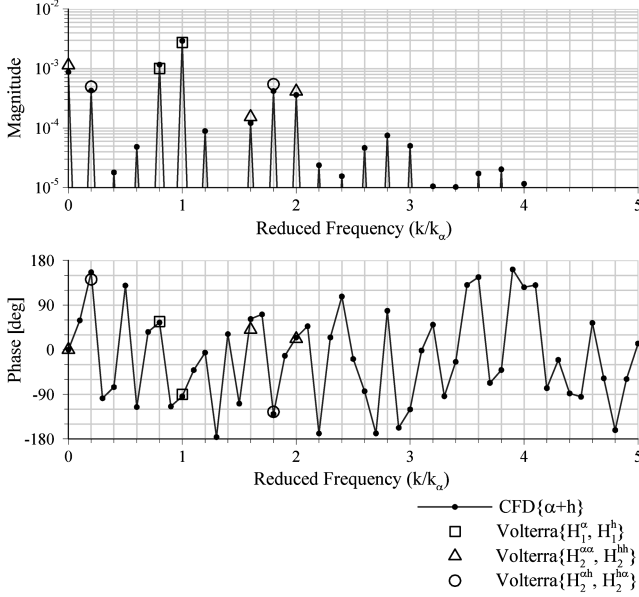| ROM	% error
Volterra $\{H_1^{\alpha}, H_1^{\dot{h}}\}$	30.6
Volterra $\{H_1^{\alpha}, H_1^{\dot{h}}, H_2^{\alpha\alpha}, H_2^{\dot{h}\dot{h}}\}$	21.7
Volterra $\{H_1^{\alpha}, H_1^{\dot{h}}, H_2^{\alpha\alpha}, H_2^{\dot{h}\dot{h}}, H_2^{\alpha\dot{h}}, H_2^{\dot{h}\alpha}\}$	12.1

**Fig. 9 Frequency content of CFD and individual Volterra kernels.**

$k/k_\alpha = 0$ (nonlinear contribution to the static response), while the cross kernels $H_2^{\alpha h}$ and $H_2^{h\alpha}$ capture the first two intermodulation harmonics $k/k_\alpha = 1.8$ (i.e., $k/k_\alpha = 1 + 0.8$) and $k/k_\alpha = 0.2$ (i.e., $k/k_\alpha = 1 - 0.8$).

C. Effect of Time Step and Impulse Magnitude on Kernel Identification Accuracy

As demonstrated by Raveh [8] and more recently by Grewal and Zimcik [24], the impulse identification method of Eqs. (24) and (25) can be very sensitive to the choice of time step and impulse amplitude. Hence, to ensure accurate Volterra kernel identification, a sensitivity analysis with respect to time step and impulse amplitude was performed. However, due to time constraints, only pitch impulse amplitude ξ_α sensitivity was analyzed. Figure 10a shows error norms for a first- and second-order Volterra ROM whose kernels were calculated using $\Delta\tau = 2$ and four different pitch impulse amplitudes: $\xi_\alpha = 0.1, 0.5, 1,$ and 2.5 deg. Here, the L^2 relative error norm is defined as

$$\%\text{Error} = \sqrt{\frac{(\text{CFD}\{\alpha\} - \text{Volterra ROM})^2}{\text{CFD}\{\alpha\}^2}} \times 100 \qquad (31)$$

where CFD$\{\alpha\}$ is the CFD output due to a pitch input as specified by Eq. (29); $\alpha = 3.16$ deg $+1$ deg $\sin(2k_\alpha\tau)$, where $M = 0.6$, $k_\alpha = 0.0811$, and $\Delta\tau = 1.96$. Observing Fig. 10a, it is clear that optimal performance is achieved with $\xi_\alpha = 0.5$ deg.
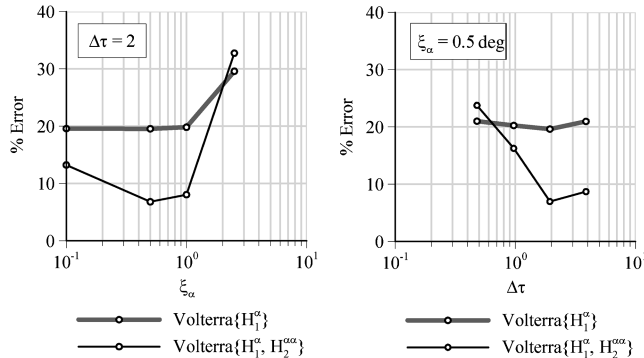
a) Volterra ROM modeling error norms vs. impulse magnitude
b) Volterra ROM modeling error norms vs. time step

Fig. 10 Sensitivity analysis of Volterra ROM accuracy with respect to time step and impulse magnitude.

Figure 10b shows error norms for a first- and second-order Volterra ROM whose kernels were calculated using $\xi_\alpha = 0.5$ deg and four different time steps: $\Delta\tau = 0.5, 1, 2$ and 4. Observing Fig. 10b, it is clear that optimal performance is achieved with $\Delta\tau = 2$.

Noting that the optimal pitch impulse amplitude of $\xi_\alpha = 0.5$ deg equals half the dynamic pitch amplitude $\bar\alpha$, it was assumed that a heave velocity amplitude $\xi_{\dot h} = 0.009 = 1/2 \cdot \dot{\bar h}$ would yield similar optimal performance. However, due to time constraints, this was not verified.

D. Effect of Pitch and Heave Frequency Separation

Figure 11 illustrates Volterra ROM error norms for inputs specified by Eq. (29):

$$\alpha = 3.16 \text{ deg} +1 \text{ deg} \sin(2k_\alpha\tau) \qquad \dot h = 0.018 \sin(2k_{\dot h}\tau) \quad (32)$$

where $M = 0.6$ and $k_\alpha = 0.0811$ for four different heave reduced frequencies: $k_{\dot h} = 0.2k_\alpha, 0.4k_\alpha, 0.8k_\alpha$ and $1.6k_\alpha$. The Volterra ROMs were calculated using the optimal parameters determined earlier: $\Delta\tau = 2, \xi_\alpha = 0.5$ deg and $\xi_{\dot h} = 0.009$. The L^2 relative error norms are defined as

$$\%\text{Error} = \sqrt{\frac{(\text{CFD}\{\alpha + h\} - \text{Volterra ROM})^2}{\text{CFD}\{\alpha + h\}^2}} \times 100 \qquad (33)$$

In all cases, inclusion of Volterra cross kernels $H_2^{\alpha\dot h}$ and $H_2^{\dot h\alpha}$ significantly improves modeling performance.

E. Curse of Dimensionality

The total CPU time t_{ID} required to identify a second-order Volterra series ROM of an N degree-of-freedom system equals

$$t_{\text{ID}} = N \cdot t_{H_1} + N^2 \cdot t_{H_2} \qquad (34)$$

where t_{H_1} and t_{H_2} are CPU times required to identify a single first-order and a single second-order Volterra kernel, respectively. Because, in general, $t_{H_2} \gg t_{H_1}$, the total identification time can become very high and render the Volterra ROM approach impractical for higher degree-of-freedom systems.

However, its possible that under certain circumstances this problem can be avoided. For example, consider the problem of transonic mode-coupling instability, flutter, of a complete aircraft configuration governed by N modal degrees of freedom. It is well known that, in many cases, the onset of flutter, and the modes involved in the instability, can be predicted using linear (dynamically linear) methods [1]. For example, linear, first-order Volterra ROMs have been demonstrated to successfully predict transonic flutter of complete aircraft configurations [3]. Identification of a second-order Volterra ROM is only necessary when the evolution of the instability is of interest, for example, determination of limit cycle oscillation amplitude and frequency. For such a scenario, it would only be necessary to identify second-order kernels corresponding to the two modes involved in the instability. Hence, the total computational time for such a model would equal
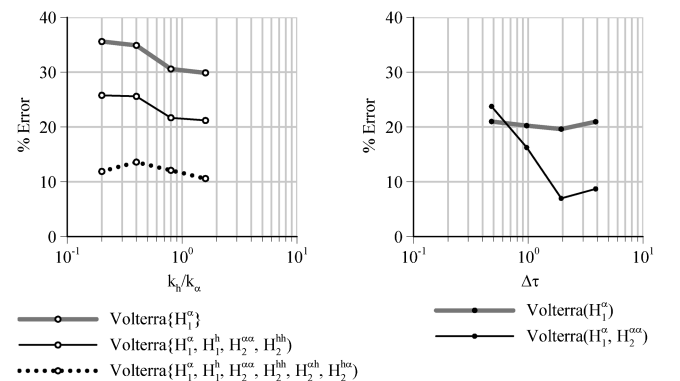

Fig. 11 Volterra ROM modeling error norms vs heave frequency.

$$t_{\mathrm{ID}} = N \cdot t_{H_1} + 2^2 \cdot t_{H_2} \qquad (35)$$

where only four second-order kernels, two direct and two cross kernels, are necessary. Identification of N first-order kernels is relatively trivial.

VII. Conclusions

The multi-input Volterra series differs from the classical Volterra series through its inclusion of cross kernels. These cross kernels capture the intermodulation harmonics when multiple degrees of freedom of a nonlinear system are perturbed simultaneously. The applicability of the multi-input Volterra series to nonlinear aerodynamic systems was demonstrated using the transonic, unsteady, two-dimensional, 2 DOF NACA 0012 airfoil. For the specific AGARD test case analyzed, the identified cross kernels significantly increased the modeling accuracy of the Volterra ROM.

References

[1] Dowell, E., Edwards, J., and Strganac, T., "Nonlinear Aeroelasticity," *Journal of Aircraft*, Vol. 40, No. 5, 2003, pp. 857–874.
doi:10.2514/2.6876

[2] Lucia, D., Beran, P., and Silva, W., "Reduced-Order Modeling: New Approached for Computational Physics," *Progress in Aerospace Sciences*, Vol. 40, 2004, pp. 51–117.
doi:10.1016/j.paerosci.2003.12.001

[3] Silva, W., "Identification of Nonlinear Aeroelastic Systems Based on the Volterra Theory: Progress and Opportunity," *Nonlinear Dynamics*, Vol. 39, No. 1–2, 2005, pp. 25–62.
doi:10.1007/s11071-005-1907-z

[4] Tromp, J. C., and Jenkins, J. E., "A Volterra Kernel Identification Scheme Applied to Aerodynamic Reactions," AIAA Paper 90-2803, Aug. 1990.

[5] Silva, W., "Application of Nonlinear Systems Theory to Transonic Unsteady Aerodynamic Responses," *Journal of Aircraft*, Vol. 30, No. 5, 1993, pp. 660–668.
doi:10.2514/3.46395

[6] Silva, W., "Reduced-order Models Based on Linear and Nonlinear Aerodynamic Impulse Responses," AIAA Paper 1999-1262, 1999.

[7] Raveh, D. E., Levy, Y., and Karpel, M., "Aircraft Aeroelastic Analysis and Design Using CFD-Based Unsteady Loads," AIAA Paper 2000-1325, 2000.

[8] Raveh, D. E., "Reduced Order Models for Nonlinear Unsteady Aerodynamics," *AIAA Journal*, Vol. 39, No. 8, Aug. 2001, pp. 1417–1429.
doi:10.2514/2.1473

[9] Silva, W., Beran, P. S., Cesnik, C. E. S., Kurdila, R. E., Prazenica, A., Librescu, R. J., Marzocca, P., and Raveh, D., "Reduced-Order Modeling: Cooperative Research and Development at the NASA Langley Research Center," International Forum on Aeroelasticity and Structural Dynamics Paper 2001-008, 2001.

[10] Lucia, D. J., Beran, P. S., and Silva, W. A., "Aeroelastic System Development Using Proper Orthogonal Decomposition and Volterra Theory," AIAA Paper 2003-1922, 2003.

[11] Silva, W., Hong, M. S., Bartels, R. E., Piatak, D. J., and Scott, R. C., "Identification of Computational and Experimental Reduced-Order Models," International Forum on Aeroelasticity and Structural Dynamics Paper 2003-US-39, 2003.

[12] Marmarelis, P. Z., and Naka, K. I., "Identification of Multi-Input Biological Systems," *IEEE Transactions on Biomedical Engineering*, Vol. BME-21, March 1974, pp. 88–101.
doi:10.1109/TBME.1974.324293

[13] Grzymacz, N. M., and Koch, C., "Functional Properties of Models for Direction Selectivity in the Retina," *Synapse*, Vol. 1, No. 5, 1987, pp. 417–434.
doi:10.1002/syn.890010506

[14] Worden, K., Manson, G., and Tomlinson, G. R., "A Harmonic Probing Algorithm for the Multi-Input Volterra Series," *Journal of Sound and Vibration*, Vol. 201, No. 1, 1997, pp. 67–84.
doi:10.1006/jsvi.1996.0746

[15] Agarossi, L., Agarossi, L., Bellini, S., Canella, A., and Migliorati, P., "A Volterra Model for the High Density Optical Disc," *Proc. IEEE International Conference on Acoustics, Speech and Signal Processing*, edited by S. Bellini, Vol. 3, IEEE Publications, Piscataway, NJ, 1998, pp. 1605–1608.

[16] Chatterjee, A., and Vyas, N. S., "Nonlinear Parameter Estimation in Multi-Degree-of-Freedom Systems Using Multi-Input Volterra Series," *Mechanical Systems and Signal Processing*, Vol. 18, 2004, pp. 457–489.
doi:10.1016/S0888-3270(03)00016-5

[17] Schetzen, M., *The Volterra and Wiener Theories of Nonlinear Systems*, Wiley, New York, 1980.

[18] Rugh, W. J., *Nonlinear System Theory. The Volterra/Wiener Approach*, John Hopkins Univ. Press, Baltimore, MD, 1981.

[19] Wiener, N., "Response of a Nonlinear Device to Noise," Radiation Laboratory, Massachusetts Inst. of Technology, Rept. 129 Cambridge, MA, 1942.

[20] "Compendium of Unsteady Aerodynamic Measurements," AGARD Tech. Rept. R-702, 1982.

[21] Tijdeman, H., and Seebass, R., "Transonic Flow Past Oscillating Airfoils," *Annual Review of Fluid Mechanics*, Vol. 12, 1980, pp. 181–222.
doi:10.1146/annurev.fl.12.010180.001145

[22] Dubuc, L., Cantariti, F., Woodgate, M., Gribben, B., Badcock, K. J., and Richards, B. E., "Solution of the Euler Unsteady Equations Using Deforming Grids," Univ. of Glasgow, Aero. Rept. 9704, 1997.

[23] Badcock, K. J., Richards, B. E., and Woodgate, M. A., "Elements of Computational Fluid Dynamics on Block Structured Grids Using Implicit Solvers," *Progress in Aerospace Sciences*, Vol. 36, No. 5, 2000, pp. 351–392.
doi:10.1016/S0376-0421(00)00005-1

[24] Grewal, A., and Zimcik, D., "Application of Reduced Order Modelling to Fluid-Structure Interaction Analysis," AIAA Paper 2008–5961, Sept. 2008.